JACS JOURNAL OF THE AMERICAN CHEMICAL SOCIETY

Article

Cite This: J. Am. Chem. Soc. 2018, 140, 4054−4061

pubs.acs.org/JACS

Tunable Thermosetting Epoxies Based on Fractionated and Well-Characterized Lignins

Claudio Gioia,*,† Giada Lo Re, Martin Lawoko,*,† and Lars Berglund

Wallenberg Wood Science Center, WWSC, Department of Fiber and Polymer Technology, KTH Royal Institute of Technology, 100 44 Stockholm, Sweden

Supporting Information

ABSTRACT: Here we report the synthesis of thermosetting resins from low molar mass Kraft lignin fractions of high functionality, refined by solvent extraction. Such fractions were fully characterized by ^{31}P NMR, 2D-HSQC NMR, SEC, and DSC in order to obtain a detailed description of the structures. Reactive oxirane moieties were introduced on the lignin backbone under mild reaction conditions and quantified by simple ^{1}H NMR analysis. The modified fractions were chemically cross-linked with a flexible polyether diamine ($M_n \approx 2000$), in order to obtain epoxy thermosets. Epoxies from different lignin fractions, studied by DSC, DMA, tensile tests, and SEM, demonstrated substantial differences in terms of thermo-mechanical properties. For the first time, strong relationships between lignin structures and epoxy properties could be demonstrated. The suggested approach provides unprecedented possibilities to tune network structure and properties of thermosets based on real lignin fractions, rather than model compounds.

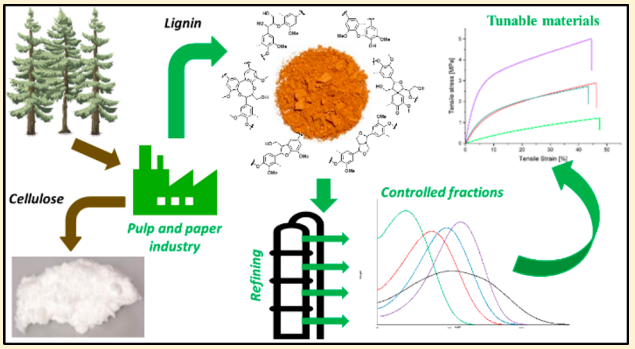

INTRODUCTION

Lignin is the most abundant resource of renewable aromatic structures and is readily available at industrial scale.[1] Industrially, it is obtained as a byproduct in the production of cellulose-rich pulp fibers. The application potential of such macromolecules includes fields such as energy,[2] chemicals,[3,4] and polymeric[5] or carbon materials.

The use of lignin in polymers has been studied empirically for a long time, in order to unravel its potential. For a comprehensive account, the reader is referred to recent reviews on efforts toward lignin applications which include the use in polymer systems,[6,7] hydrogels,[8] nanoparticle and composite systems,[9] carbon fibers,[10] and thermoplastics[11] to mention but a few. Despite these efforts, the industrial breakthrough for large-scale polymer materials based on lignin has still not taken place, partly due to difficulties associated with the heterogeneity and impurity of industrial lignin. Yet, the aromatic backbone is attractive and should confer rigidity to macromolecular structures, more so than many other biobased building blocks, such as fatty acids[12] and terpenes.[13]

The synthesis of biobased thermosets represents a promising field for lignin utilization. The presence of functional groups such as phenols, aliphatic hydroxyls, and carboxylic acids favors chemical modification of lignin. Specific moieties essential for chemical cross-linking (curing) of oligomers or prepolymers can be introduced. In addition, the aromatic nature of lignin may constitute a natural and sustainable alternative to petrol-based compounds such as terephthalic acid or bisphenol A, where there are concerns from the environmental and health point of view.[14,15]

Epoxy resins are one of the major classes of thermosets with a market value that will reach $25.8 billion in 2018 and an estimated value of $33.6 billion in 2022.[16] Their applications include coatings and adhesives of high performance. The control of the properties is based on the tuning of the chemical structure and cross-linking of the main components, resulting into a versatile class of materials. The amine curing process is well understood and reliable, with limited risk for undesired side reactions.

As a consequence of the need for sustainable development, there are significant efforts on biobased alternatives to substitute petrol-based components of epoxy resins.[17] Lignin represents a promising feedstock for both aromatic monomers[18] and macromolecular structures. Although its statistical chemical structure and polydispersity are limiting the properties of the final materials, in order to overcome such issues, lignin from mild plant extraction processes, such as organosolv,[19] hydrolysis,[20] hydrogenolysis,[21] or partial depolymerization,[22] have been preferred in material science efforts. The reason is relatively low polydispersity, however, none of those lignins are currently available in large scale in contrast with industrial Kraft lignin. Another approach is the exploitation of a purified fraction of the lignin.[23] Although such an approach produces a

Received: December 23, 2017
Published: March 2, 2018

DOI: 10.1021/jacs.7b13620
J. Am. Chem. Soc. 2018, 140, 4054−4061

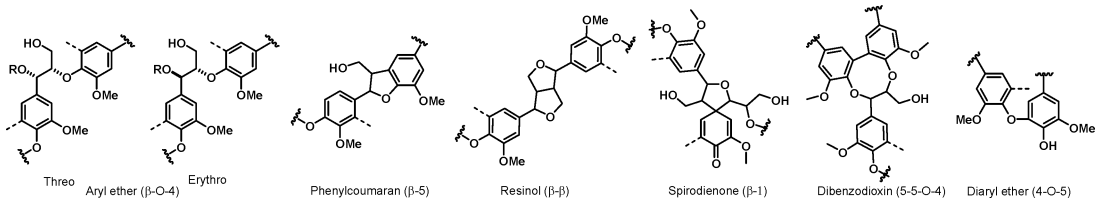

Figure 1. Main interunit structures present in native lignin.

Table 1. Characterization of the Parent Lignoboost Kraft Lignin and of the Fractions Obtained by Solvent Extraction

	M_w[a] (g/mol)	Đ[a]	DP[b]	yield (%)[c]	aliphatic OH (mmol/g)[d]	COOH (mmol/g)[d]	phenols (mmol/g)[d]	C5-cond. phenols (%)[d]
error					±0.1	±0.1	±0.5	
KL	6800	6.1	–	–	1.4	0.4	4.4	43
LF_{EtOAc}	1000	1.5	4	14	1.0	0.9	6.8	28
LF_{EtOH}	2100	1.9	6	37	1.3	0.6	4.7	40
LF_{MeOH}	3200	2,0	8	7	1.6	0.3	4.4	45
$LF_{Acetone}$	5400	2.0	13	8	1.6	0.3	4.5	50
residual	17700	2.8	–	34	2.1	0.3	3.5	52

[a]Molar mass analysis by SEC. [b]Calculated by elemental analysis and SEC data. [c]Isolated yields. [d]Quantified by ^{31}P NMR.

more homogeneous starting material with lower polydispersity, there is still a lack of deep systematic investigations relating chemical structure and molecular weight of lignin to thermoset properties.

The presence of different functionalities and repeat units in lignin, as well as the molecular weight variations and polydispersity, needs to be analyzed in order to design and tune the properties of lignin-based thermosets. The present study aims to show a route toward fractionation, characterization, and selective functionalization of industrial lignins, so that molecular-scale control can be exercised for lignin-based thermoset polymers. The large variation in functional groups and interunit linkages in lignin is mainly a consequence of the biosynthesis process and the severity of the extraction process to isolate lignin.

In biosynthesis, the initiation of polymerization occurs by a mild enzymatic oxidation of phenolic monomers to form phenoxy radicals and their resonances. In a first stage, a favorable radical coupling to dimers results in a quinone methide intermediate, an electrophile, permitting nucleophilic addition reactions in a second step. The resonance stabilized radicals allow the formation of different types of interunit linkages such as aryl ether (*β*-O-4), phenylcoumaran (*β*-5), resinol (*β*-*β*), spirodienone (*β*-1), dibenzodioxin (5-5-O-4) and as reported in Figure 1. Of these reported, the aryl ether linkage dominates in native lignins. The relative amounts of the linkages however also vary between different species. A modern conflicting point is whether native lignin is highly branched, as suggested by Adler,[24] or relatively linear. Recent works suggests the latter.[25,26]

The extraction process applied to retrieve lignin is responsible for major structural modifications of native lignin. The Kraft technology for industrial production of unbleached cellulosic Kraft pulp, produces 70 Mtons/year of lignin-rich byproducts. Most of this is incinerated, and cooking chemicals are recovered. The process uses high temperature (170 °C) and hydrogensulfide and hydroxyl anions in order to cleave the main lignin backbone, consisting mainly of the aryl ether (*β*-O-4) bond. This results in decreased molecular weight and increased phenolic hydroxyl content. Both factors enhance lignin solubility under alkaline conditions. Other reactions include the introduction of sulfur-based moieties, production of formaldehyde, and creation of new linkages such as condensed phenols or stilbene-like structures. As a result, Kraft lignin is a broad polydisperse mixture of heterogeneous structures. A recent publication by Crestini and co-workers presents the detailed structural motifs of kraft lignin, clearly demonstrating heterogeneity in such substrates.[27] The structures make it clear that lignins need to be purified by fractionation in order to be suitable for material applications.[27] Since criteria for tunable and reproducible epoxy resin precursors include homogeneity and narrow polydispersity, Kraft lignin considered for this purpose needs to be fractionated and functionalized.

The objective of this work, is to study effects of chemical and macromolecular structures of well-defined and well-characterized industrial lignin fractions on the thermo-mechanical properties of lignin-based epoxy resins. An industrial softwood lignin is refined in order to isolate reproducible and fully characterized lignin fractions. Such materials were chemically modified by epoxidation under mild conditions, in order to preserve the basic lignin structures. Epoxidized lignins were then cross-linked with an industrial diamine. Thermo-mechanical properties of the resulting epoxy thermosets are analyzed in order to establish a correlation with the initial structures. The possibility to tune the properties of lignin-based epoxy resins is illustrated through effects from lignin fraction selection. These achievements have not previously been demonstrated for epoxies based on real, industrial-quality lignin and suggests a strategy for studies supporting longer-term industrialization of lignin-based thermosets. In previous work, lignin fractionation, characterization, and functionalization of lignin precursors have not been carried out in a sufficiently controlled manner, leading to slow progress with respect to molecular-scale understanding of lignin thermosets.

RESULTS AND DISCUSSION

Refining Lignin. Initial studies showed that spruce Kraft lignin, retrieved from black liquor by the Lignoboost technology (KL), consists of a heterogeneous mixture with respect to both structure and molar mass (polydispersity index (Đ) of 6.1 (Table 1, Supporting Information Figure S1).

The fractionation process developed in our laboratory[6] involved sequential extraction using organic solvents such as

DOI: 10.1021/jacs.7b13620
J. Am. Chem. Soc. 2018, 140, 4054−4061

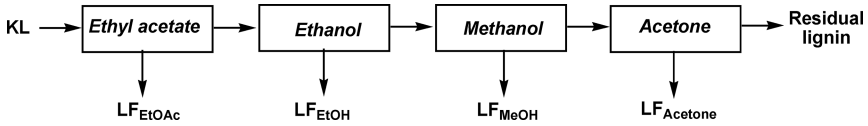

Figure 2. Schematic description of the sequential refining approach.

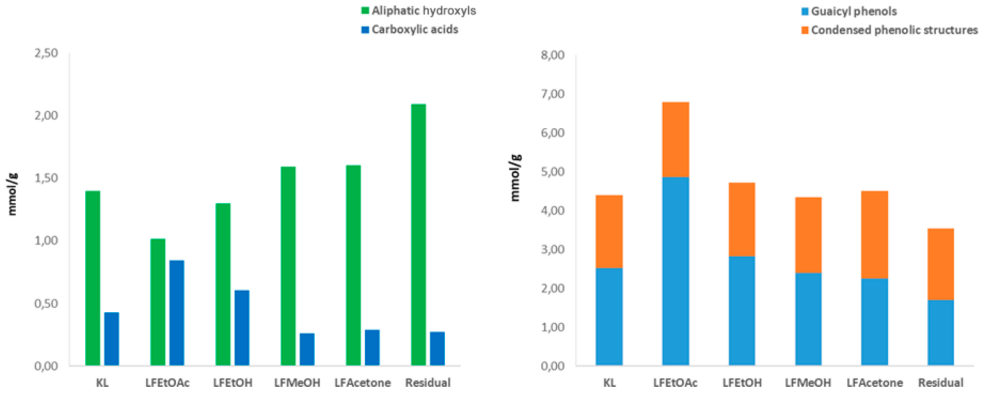

Figure 3. Semiquantification of aliphatic alcohols and carboxylic acid in the fractions (left) and quantification of different phenolic structures (right), obtained by ^{31}P NMR.

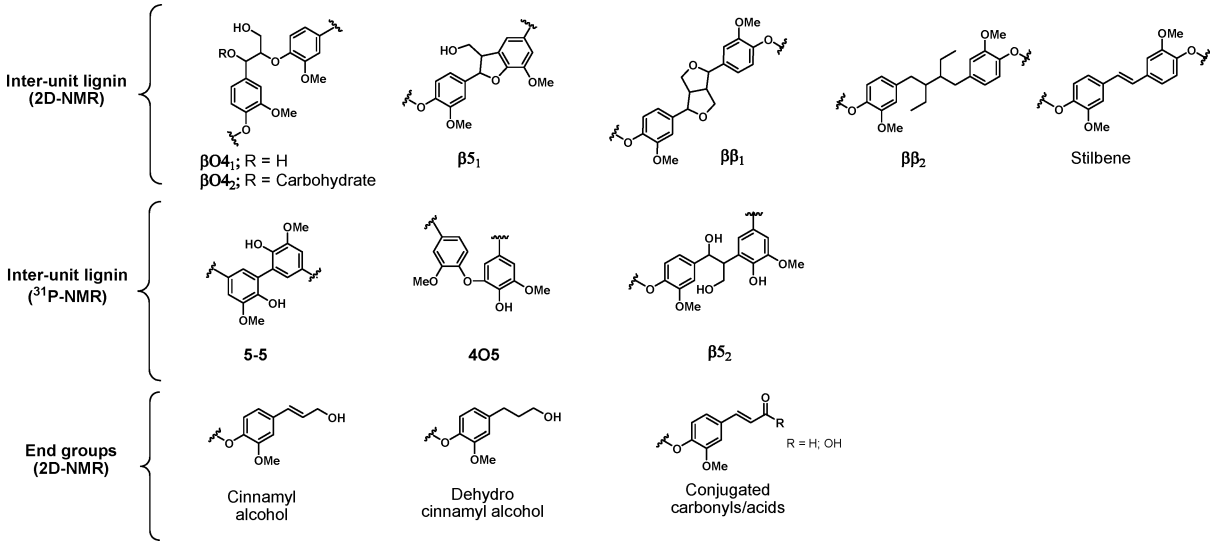

Figure 4. Main structures detectable by HSQC and ^{31}P NMR.

ethyl acetate (EtOAc), ethanol (EtOH), methanol (MeOH), and acetone (Figure 2). These solvents have all been listed as easily recoverable, green, and sustainable.[28] The sequence of extraction was designed in order to retrieve fractions with low polydispersity and gradually increasing molecular weight. As reported in Table 1, LF_{EtOAc} constitutes the lower M_w fraction of short chains with an average degree of polymerization (DP) of 4 units, while the largest $LF_{Acetone}$ presents a M_w of about 5400 and a DP of 13 units.

The polydispersity of all the retrieved fractions is between 1.5 and 2.8, which is suitable for thermoset precursors. This was recently demonstrated in the synthesis of thiol−ene resins from refined lignin.[29] Regarding the yields, the first two fractions (LF_{EtOAc} and LF_{EtOH}) account for approximately 50%, while LF_{MeOH} and $LF_{Acetone}$ present more moderate yields (7−8%). A residue was recovered at the end of the process, having a 34% yield. It required more polar and less sustainable solvents such as DMSO and DMF or pyridine, which made this fraction less suitable for further chemical modification.

^{31}P NMR and 2D-NMR Analysis of Lignin Fractions. The purpose is to characterize the detailed lignin structure, as input for the next stage, where a polymer material is created. For each fraction, a detailed analysis of the main functional groups was performed by ^{31}P NMR (Table 1). As reported in Figure 3, the amount of carboxylic acids is decreased with increasing M_w of the fractions, whereas the number of aliphatic alcohols is increased. The reason is extensive oxidation, which transformed the aliphatic alcohols into carboxylic acid during the Kraft process. Note that aliphatic alcohols are usually located in the side chains of lignin.

Such oxidation is also more likely to occur at end groups, an argument supported by the higher content of acidic groups in the lower M_w fractions, that is, LF_{EtOAc} and LF_{EtOH}. Figure 3 displays the distribution of noncondensed and C5-condensed phenolics on guaiacyl moieties. The noncondensed phenols

DOI: 10.1021/jacs.7b13620
J. Am. Chem. Soc. 2018, 140, 4054−4061

represent the terminal groups of the oligomers. The C5-condensed structures are mainly from the native lignin structure and are enriched during the pulping. A small fraction may result from reactive recombination of shorter molecules imposed by the harsh conditions of the Kraft process.[30] As reported in Table 1, the percentage of condensed phenols is higher in high M_w fractions.

The macromolecular backbone of the fractions and the nature of the linkages connecting the monomers were studied combining ^{31}P NMR and 2D-HSQC analysis. As reported in Figure 4, a variety of different structures were detected. In particular, the nature of the connecting units will influence the rigidity of the macromolecular structure. Linkages such as $\beta O4_1$, $\beta O4_2$, $\beta\beta_2$, and $\beta 5_2$ are likely to confer flexibility, while interconnections such as $\beta 5_1$, $\beta\beta_1$, 5-5, and 4O5 may impart higher rigidity since their hindered structures will prevent free rotation.

Table 2 reports the percentage of the main interunit linkages in the different fractions. As expected, all the fractions show

Table 2. Quantification of the Most Occurring Inter-Unit Linkages and Terminal Groups

interunit	LF_{EtOAc} (%)	LF_{EtOH} (%)	LF_{MeOH} (%)	$LF_{Acetone}$ (%)
($\beta O4_1$)[a]	2	5	8	11
($\beta O4_2$)[a]	1	1	2	3
($\beta 5_1$)[a]	1	2	3	4
($\beta\beta_1$)[a]	3	3	6	11
($\beta\beta_2$)[a]	3	3–4	3	2
stilbene[a]	4–6	4–6	5	6
(5-5; 4O5; $\beta 5_2$)[b]	35	35	36	41
end groups[a]				
cinnamyl alcohol	<1	1	1	<1
dihydro cinnamyl alcohol	6	5	3	3
conjugated carbonyls/ acids[c]	18	11	6	6

[a]Semiquantified by HSQC (the end group percentage may be overestimated). [b]Quantified by ^{31}P NMR. [c]Overlapping signals difficult to discriminate.

significant modification compared with the native structure. For example, the $\beta O4$ interunits are only between 2–11% in contrast with about 45% typical for the native structure.[31] The most common interunit linkages are C5-condensed phenolic structures (5-5; 4O5; $\beta 5_2$), and they represent 35–41% of the interunit linkages of the fractions. The dramatic decrease in BO4 type structures is expected since these are favorably cleaved during the pulping, with concomitant formation of new phenolic ends, which yields smaller molecules.[27] The high content of the C5 linked lignins can be explained by two mechanisms. The first is the stability of the C–C bonds between two aromatic moieties during Kraft pulping, and this results in enrichment of these structures. The second is the formation of new linkages through radical coupling chemistry initiated by the production of elemental sulfur in Kraft pulping.[32] This second reaction is also the origin of branching in Kraft lignins.[27] $\beta\beta_1$ and stilbene structures are equally distributed in all the fractions, while the content of all the other linkages ($\beta O4_1$, $\beta O4_2$, $\beta 5_1$, $\beta\beta_1$) tends to increase with the molecular weight of the fractions. The stilbene structures are formed from the cleavage of C_β-C_γ linkage in $\beta 1$ or $\beta 5$ structures, leading to unsaturation and release of formaldehyde.[33] This expands the functionality portfolio of Kraft lignins to include C=C double bonds, in addition to phenolic and aliphatic hydroxyls.

Kraft lignins show characteristic end groups in the form of conjugated carbonyls.[27] The present results for end groups, obtained with 2D-NMR analysis, are in accordance with the data obtained from ^{31}P NMR. We observe a decrease in total amount of terminal groups as the M_w is increased. Furthermore, oxidation is more common in fractions with lower M_w.

On the basis of the reported results, including different degrees of polymerization, DP (Table 1), we can establish a qualitative description of the different fractions. The short LF_{EtOAc} and LF_{EtOH} have more heterogeneous chemical variability, but the polydispersity of these fractions is lower. They have stiff structures mainly consisting of condensed phenolic interunits. LF_{MeOH} and $LF_{Acetone}$, present higher variability in terms of interunit linkages in the same chain, constituting both flexible and stiff (condensed) moieties. These molecular properties are important and will be revisited in the context of thermoset properties.

Synthesis and Characterization of Lignin-Based Thermosets. Oxirane moieties were introduced with a glycidylation method through the reaction of epichlorohydrin with the different lignin fractions (Scheme 1). In particular, this step was optimized for mild conditions in order to prevent undesired cleavage or aggregation of the lignin backbone structure. Acetone/water 50:50 was found to be an excellent solvent system for all the fractions at 50 °C. Parameters such as amount of sodium hydroxide and reaction time were optimized to maximize the functionalization of sites such as phenols, carboxylic acids, and aliphatic alcohols (see SI Table S1). Table 3 reports molecular weight of the modified fractions. When compared to the original fractions (cf. Tables 1 and 3), a slight increase in M_w is observed, which reflects increased mass from chemical modification. The polydispersity is not significantly changed by the epoxidation, which means that extensive degradation or macromolecular aggregation is not taking place.

Scheme 1. Introduction of Oxirane Moieties on Lignin

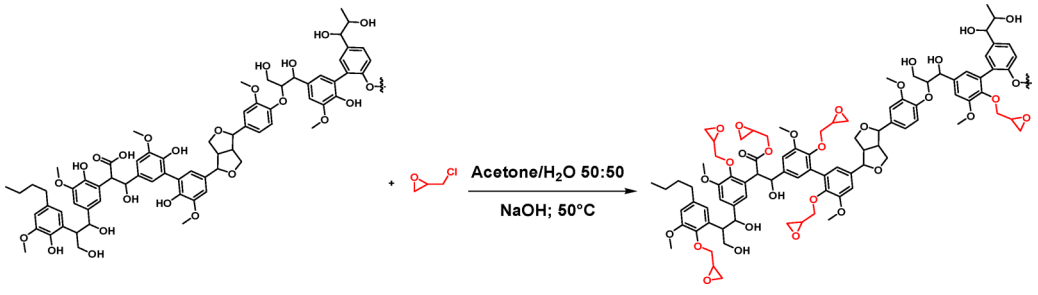

DOI: 10.1021/jacs.7b13620
J. Am. Chem. Soc. 2018, 140, 4054–4061

Table 3. Characterization of the Epoxidized Fractions and Formulation of thermosets

lignin epoxy fraction	M_w[a]	Đ[a]	oxirane content (mmol/g)[b]	epoxy lignin content (%)[c]
Epoxy-LF_{EtOAc}	1200	1.6	3.9	33.3
Epoxy-LF_{EtOH}	2900	2.3	3.2	37.7
Epoxy-LF_{MeOH}	4500	2.3	3.1	38.5
Epoxy-$LF_{Acetone}$	5900	2.4	2.7	41.8

[a]Molar mass analysis by SEC. [b]Quantified by ^{1}H NMR using 4-nitro benzaldehyde as internal standard. [c]Content of lignin in the formulation expressed in weight percent; the ratio was designed to maintain the stoichiometric ratio 2:1 oxirane/amine

^{31}P NMR analysis of the epoxidized fractions shows complete consumption of the acid and phenolic moieties due to their high reactivity in basic conditions (Figure 5). In contrast, the aliphatic alcohol signals were increased. A new strong aliphatic signal is observed between 145 and 146 ppm. This signal is likely to originate from the NMR-phosphite derivatization of the phenolic-linked epoxide.[34] Alternatively, it could result from the hydroxyls introduced on the structure by the incomplete formation of the oxirane ring after the addition of epichlorohydrin. Mechanisms for these scenarios are provided in the SI (Figure S20).

2D-HSQC analysis confirmed the introduction of the oxirane ring on lignin (Figure 6, SI Figures S22−25). Furthermore, no significant alteration of the main interunit linkages is observed, implying that the integrity of the lignin skeleton is maintained during epoxidation. Because of the peak resolution obtained by HSQC, it was also used to identify the least overlapping signal of the inserted epoxy group which in turn would be used for quantification in proton NMR, that is, the C/H correlation peak at 43.1/2.8 ppm. Such signals overlap only with low intensity peaks producing a minimal over estimation in the final quantification. Thus, the signal at 2.8 ppm in the ^{1}H NMR analysis was applied for quantification with *para*-nitro benzaldehyde as internal standard, according to the procedure described in the SI. As reported in Table 3, the amount of oxirane content is highest in Epoxy-LF_{EtOAc} with 3.9 mmol of epoxy groups/gram of lignin, and this progressively decreases with increased M_w of the lignin fractions (down to 2.7 mmol/g for Epoxy-$LF_{Acetone}$). This tendency is mainly related to the increase in functional group concentration (mainly phenols and carboxylic acids) with decreased molar mass.

Polyetheramine D2000 was selected as cross-linking agent ($M_w \approx 2000$) to cure the epoxidized lignin fractions. This diamine also confers ductility and lowered T_g to the resin, while lignin promotes high Young's modulus and increased glass transition temperature T_g. In addition, the poly(propylene oxide) chain of Polyetheramine may interact with the polar groups of lignin and favor dissolution and homogeneous mixing. In preliminary tests, mixing problems were observed when a lower molar mass polyetheramine (D400) was used. The choice of amine, with respect to molar mass, is therefore important for mutual solubility, with the higher molar mass favorable in this particular case. Finally, the length of the diamine was designed in order to create a more flexible molecular network in the thermoset.

Table 3 reports the initial formulations used to obtain the thermosets based on the epoxidized lignin fractions. The amount of diamine was tuned in order to maintain a stoichiometric ratio between number of epoxy and amine groups, that is, two oxirane moieties for each NH_2 group. A solution of epoxidized lignin fractions and polyetheramine D2000 in acetonitrile was cast in Teflon molds. The curing procedure involved 1 h at 50 °C in order to remove the solvent, 2 h at 100 °C, and postcuring at 150 °C for 2 additional hours. This cure cycle was optimized according to the thermal curing profile obtained by DSC experiments (see SI, Figure S30). In Figure 7 are reported, as an example, the FTIR spectra of LF_{EtOAc}, Polyetheramine D2000, Epoxy-LF_{EtOAc}, and Resin 1. The presence of the oxirane ring is confirmed in the modified resins by the appearance of medium weak bands at 907 and 755 cm^{-1}. Furthermore, the reduction of the intensity of the OH signals at 3300 cm^{-1} supports the consumption of phenolic moieties due to epoxidation. The effectiveness of the curing conditions is supported by the disappearance of the band at 755 cm^{-1}, while the signal at 907 cm^{-1} is overlapping with the band

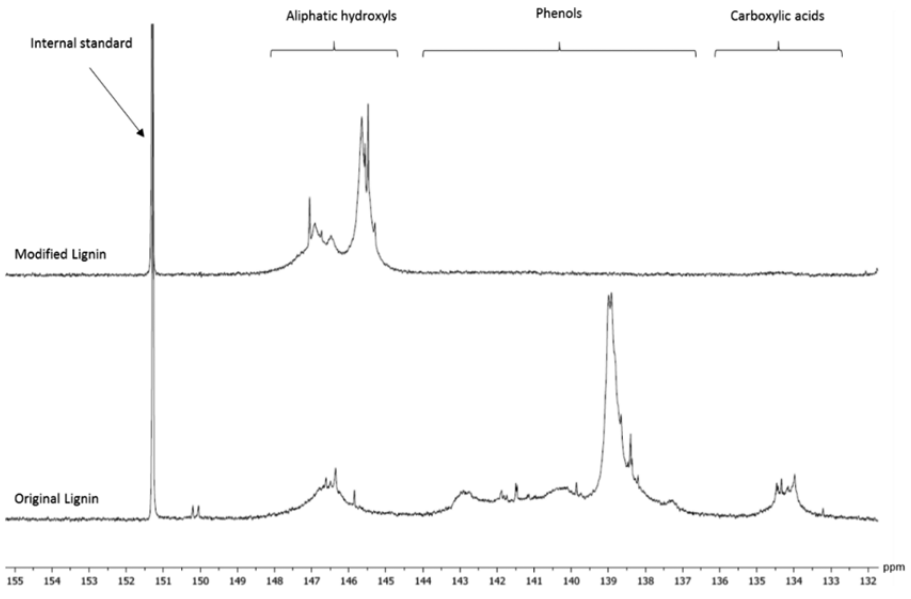

Figure 5. ^{31}P NMR of the pristine LF_{EtOAc} (bottom) compared with Epoxy-LF_{EtOAc} (top).

DOI: 10.1021/jacs.7b13620
J. Am. Chem. Soc. 2018, 140, 4054−4061

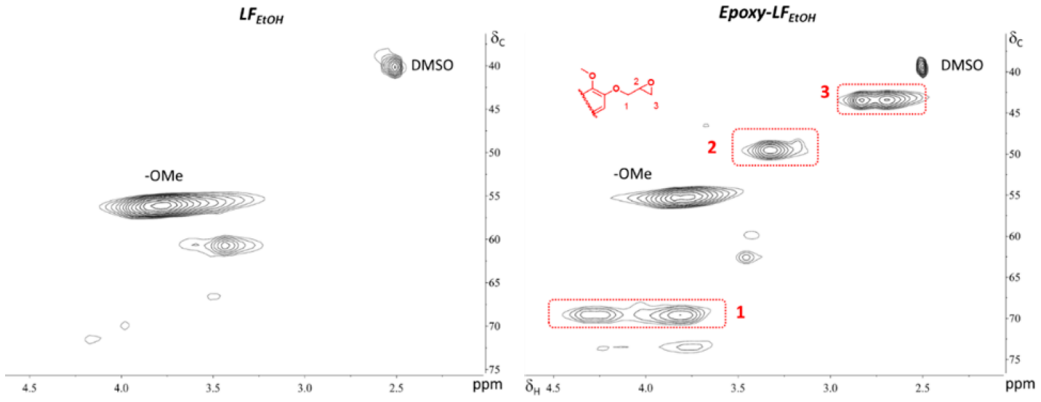

Figure 6. HSQC analysis of the pristine LF$_{EtOH}$ (left) compared with Epoxy-LF$_{EtOH}$ (right).

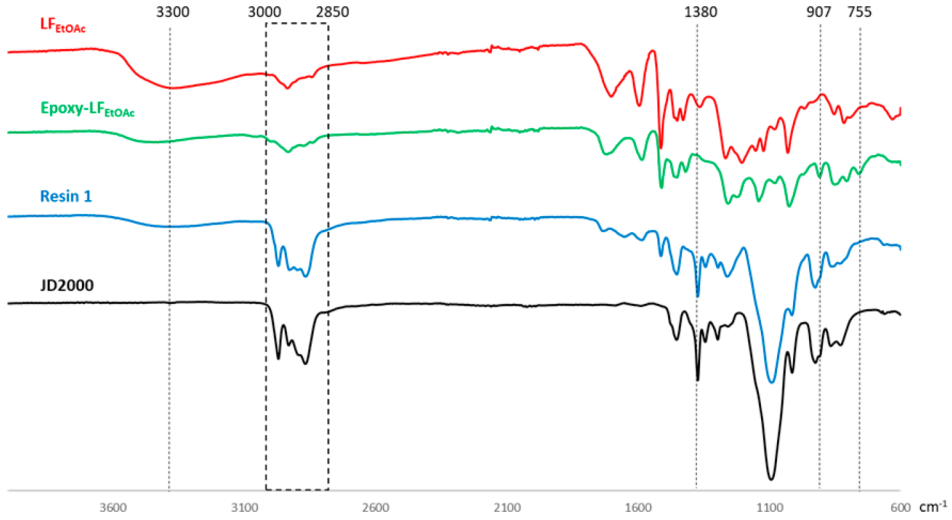

Figure 7. FT-IR respectively of LF$_{EtOAc}$, Epoxy-LF$_{EtOAc}$, Resin 1, and Polyetheramine D2000.

related to the C−N bonding.[35] The new bands observed between 3000 and 2850 and the signal at 1380 are, respectively, related to the stretching of the alkyl groups and −CH$_3$ bending of the Jeffamine PPO structure.[35]

The thermal behavior of the resins was evaluated by DSC analysis and compared with the thermal properties of the corresponding lignin fractions. As reported in Table 4, the four fractions show increased T_g, starting from 74.5 °C of LF$_{EtOAc}$ to 190.4 °C of LF$_{Acetone}$. This trend reflects increasing M_w of the fractions, since this lowers molecular mobility. All the obtained thermosets appear to be homogeneous materials presenting a single T_g, at about −50 °C (see SI, Figure S32), indicating a strong contribution from the polyetheramine, and a significant polyetheramine-rich phase. The observation of a unique thermal transition for all the resins with intermediate values between lignin (74−190 °C) and polyetheramine (−71 °C, see SI, Figure S31) is in support of fully reacted thermosets.

Table 4. Thermal Behavior of Lignin Fractions Compared with Thermo-Mechanical Behavior of the Corresponding Thermosets

lignin fractions			thermosets			
	T_g (°C)[a]	ΔC_p (J/g °C)[a]		T_g (°C)[a]	ΔC_p (J/g °C)[a]	T_α[b]
LF$_{EtOAc}$	74	0.48	Resin 1 (from LF$_{EtOAc}$)	−50	0.37	−52
LF$_{EtOH}$	132	0.42	Resin 2 (from LF$_{EtOH}$)	−50	0.22	−53
LF$_{MeOH}$	169	0.32	Resin 3 (from LH$_{MeOH}$)	−51	0.26	−54
LF$_{Acetone}$	190	0.45	Resin 4 (from LF$_{Acetone}$)	−52	0.20	−51

[a]Calculated by DSC analysis. [b]Calculated by DMTA analysis.

Dynamic mechanic thermal analysis (DMTA) was used to investigate relaxation transitions and modulus changes of the different lignin-based resins. As reported in Table 4, all thermosets show one α transition temperature of around $T_\alpha \approx -50$ °C, determined according to the standard ASTM D4092-07 as the peak of the loss modulus curve, in agreement with the glass transition detected by DSC.[36] The changes in the storage and loss moduli (E' and E'') as a function of temperature are presented in Figure 8. In Table 5, the main properties from DMTA and tensile tests are reported. The storage modulus of lignin-based resins is found to follow two different trends, discriminated by their glass transition temperature. In the glassy state, the resin prepared from the EtOAc fraction, with the lower molecular weight, shows a significantly higher storage modulus compared to the other thermosets. The elastic storage moduli at −100 °C for Resins 1, 2, 3, and 4 are 5960, 4360, 4015, and 3890 MPa, respectively (see Table 5).

The lower the molecular weight of the corresponding lignin fraction, the higher the storage modulus in the glassy state of the cured network. The rigidity of the system is influenced by

DOI: 10.1021/jacs.7b13620
J. Am. Chem. Soc. 2018, 140, 4054−4061

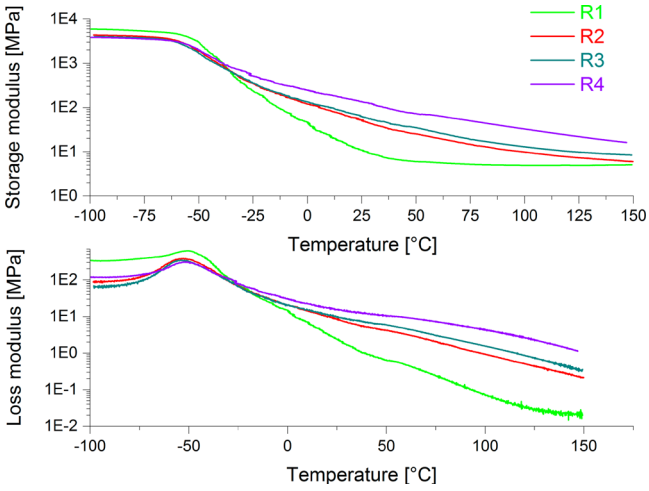

Figure 8. Representative log plot of the storage and loss moduli as a function of the temperature recorded during the DMTA analysis of the different cured lignin-based epoxy resins.

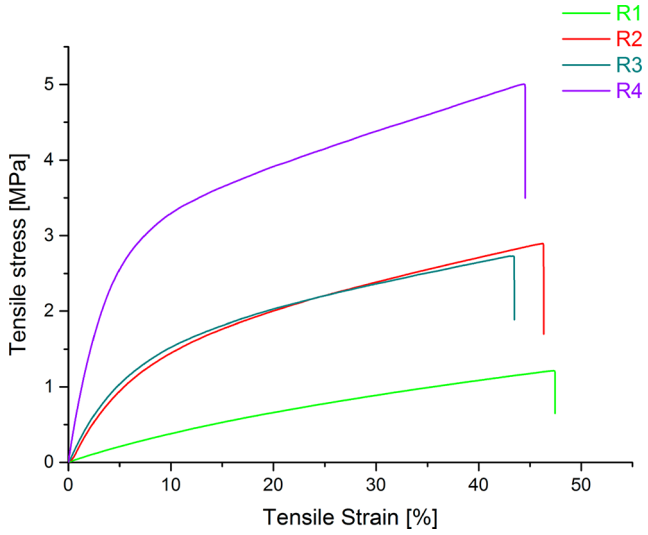

Figure 9. Representative tensile stress−strain curves of the different cured lignin-based epoxy resins.

the cross-link junctions of the epoxy bridges, which are more efficient with the lower molecular weight lignin fraction. Possibly, the packing of the network and the free volume are lower in thermosets based on lower molecular weight lignin. Above the softening temperature of the glass transition (Figure 8), an inversion of the trend occurs. The higher the molecular weight of the lignin fraction, the higher the elastic storage moduli of the corresponding soft epoxy resins. When the temperature is raised to room temperature, the elastic storage modulus of epoxy-bridged Resin 4 still is 156 MPa, but the elastic storage moduli for the Resins 3, 2, and 1 have decreased to 73, 60, and 13 MPa, respectively. Such results indicate that the epoxy from $LF_{Acetone}$ retains higher thermo-mechanical properties at high temperature due to the higher stiffness of the lignin fraction with the higher molecular weight. The segmental mobility in a polymer around a cross-link junction is reduced for both branched and cross-linked polymers, regardless of the mobility of the chain end far from the branch point.[37] Branched macromolecules show higher glass temperatures compared with their linear analogs due to steric hindrance and the corresponding more complex deformation mechanisms.[38,39] The motion restriction decreases the dissipation of energy stored, resulting in higher elastic storage modulus shown by increasing molecular weight of the resin. The trend observed suggested possible contribution of intermolecular interactions to the elastic free energy of the network at equilibrium, and consequently to its storage modulus, meaning that the assessment of the cross-linking density by adopting the Wall−Flory model of the rubber elasticity theory is not valid for the considered system.[40] Tensile tests were carried out on the different epoxy-bridged resins, and their representative stress−strain behaviors are reported in Figure 9. The Young's moduli of the lignin-based soft epoxy resins range from 6 to 100 MPa, following the trend already observed for the storage modulus in dynamic experiments. Above −50 °C, the stiffness of material is controlled by the lignin fraction. Possibly, the increasing ratio of condensed interunit linkages in the higher M_w fractions may be significant. The tensile strength of the resins varied from 1.2 to 5.0 MPa and increases with the molecular weight of the lignin fraction. Strain to failure are almost insensitive to the structure of the starting materials.

It is worth noting the similarity of the stress−strain curves of Resins 2 and 3 and the fact that they have similar molecular weight. The mechanical properties of the resins could therefore be tuned by control of the molecular weight of the lignin fraction.

The fracture surfaces from tensile tests of cured epoxy resins were analyzed by scanning electron microscopy (SEM) (Figure S34 in SI). The SEM images illustrate that each epoxy resin composition has one-phase morphology on the micrometric scale.[41] The fracture surface of Resin 1 is less smooth in comparison to the other epoxy resins. The higher magnification of Resin 4 showed a submicronic granular morphology. A submicrometric domain cannot be excluded. Secondary transitions were indeed observed in the curves of tan δ for Resin 4 suggesting nanometric domains, which may also be present in other compositions.

CONCLUSION

Despite the fact that chemical complexity and inherent heterogeneity usually imply a relatively empirical use of lignin in material synthesis, for the first time we investigated the possibility to control lignin on molecular level to tailor the

Table 5. Main Mechanical Properties Assessed by DMTA and Tensile Tests of the Different Lignin-Based Epoxy Resins

sample	E'(−100 °C) [MPa][a]	E'(20 °C) [MPa][a]	E_{young} [MPa][b]	σ_{break} [MPa][b]	ε_{break} [%][b]
Resin 1	5960 ± 50	13 ± 0.3	6 ± 0.05	1.2 ± 0.06	47 ± 2.0
Resin 2	4360 ± 40	60 ± 1	20 ± 0.1	2.9 ± 0.12	47 ± 1.8
Resin 3	4015 ± 50	73 ± 1	24 ± 0.1	2.7 ± 0.10	43 ± 1.7
Resin 4	3890 ± 30	156 ± 2	100 ± 0.7	5.0 ± 0.20	44 ± 1.5

[a]Calculated by DMTA analysis. [b]Calculated by tensile test.

DOI: 10.1021/jacs.7b13620
J. Am. Chem. Soc. 2018, 140, 4054−4061

thermo-mechanical properties of the final materials. To achieve that, Kraft lignin was refined into four well-characterized fractions, defined by low polydispersity and increasing molecular weight. Subsequently, they were functionalized by means of a selective epoxidation reaction, and the extent of functionalization was quantified by ^{1}H NMR to allow a stoichiometric formulation of the thermosets. The curing was performed with an aliphatic diamine using a well-known reaction mechanism to successfully obtain a three-dimensional network. The mechanical properties of the materials demonstrated a strong improvement with higher molecular weight fractions. Finally, the T_g of the materials was clearly dominated by the flexible amine, suggesting the possible formation of amine and lignin dominated domains.

■ ASSOCIATED CONTENT

Supporting Information

The Supporting Information is available free of charge on the ACS Publications website at DOI: 10.1021/jacs.7b13620.

General details on the material and methods, full characterization of lignin fractions, optimization of the conditions of epoxidation, full characterization of the modified fractions, study of the curing conditions, and thermal characterization of the final materials (PDF)

■ AUTHOR INFORMATION

Corresponding Authors

*cgioia@kth.se

*lawoko@kth.se

ORCID

Claudio Gioia: 0000-0001-8483-7622

Giada Lo Re: 0000-0001-8840-1172

Martin Lawoko: 0000-0002-8614-6291

Author Contributions

†These authors contributed equally.

Notes

The authors declare no competing financial interest.

■ ACKNOWLEDGMENTS

The authors are grateful to the Knut and Alice Wallenberg Foundation for financial support through the Wallenberg Wood Science Center at KTH Royal Institute of Technology.

■ REFERENCES

(1) Kendal Pie, K. In *Biorefineries – Industrial processes and products; Industrial lignin production and applications*; Kamm, B., Gruber, P. R., Kamm, M., Eds.; Wiley VCH, Verlag GmbH& Co: Weinheim, 2006. Ragauskas, A. J.; Beckham, G. T.; Biddy, M. J.; Chandra, R.; Chen, F.; Davis, M. F.; Davidson, B. H.; Dixon, R. A.; Gilna, P.; Keller, M.; Langan, P.; Naskar, A. K.; Saddler, J. N.; Tschaplinski, T. J.; Tuskan, G. A.; Wyman, C. E. *Science* **2014**, *344*, 1246843.

(2) Kruse, A.; Funke, A.; Titirici, M. *Curr. Opin. Chem. Biol.* **2013**, *17*, 515.

(3) Zhang, Z.; Song, J.; Han, B. *Chem. Rev.* **2017**, *117*, 6834.

(4) Ma, Z.; Custodis, V.; Hemberger, P.; Bährle, C.; Vogel, F.; Jeschk, G.; Van Bokhoven, J. A. *Chimia* **2015**, *69* (10), 597.

(5) Naseem, A.; Tabasum, S.; Zia, K. M.; Zuber, M.; Ali, M.; Noreen, A. *Int. J. Biol. Macromol.* **2016**, *93*, 296.

(6) Duval, A.; Vilaplana, F.; Crestini, C.; Lawoko, M. *Holzforschung* **2015**, *70* (1), 11.

(7) Laurichesse, S.; Huillet, C.; Avérous, L. *Green Chem.* **2014**, *16* (8), 3958.

(8) Thakur, V. K.; Thakur, M. K. *Int. J. Biol. Macromol.* **2015**, *72*, 834.

(9) Norgren, M.; Edlund, H. *Curr. Opin. Colloid Interface Sci.* **2014**, *19* (5), 409.

(10) Fang, W.; Yang, S.; Wang, X.-L.; Yuan, T.; Sun, R.-C. *Green Chem.* **2017**, *19*, 1794.

(11) Wang, C.; Kelley, S. S.; Venditti, R. A. *ChemSusChem* **2016**, *9* (8), 770.

(12) Biermann, U.; Bornscheuer, U.; Meier, M. A. R.; Metzger, J. O.; Schäfer, H. J. *Angew. Chem., Int. Ed.* **2011**, *50* (17), 3854.

(13) Winnacker, M.; Rieger, B. *ChemSusChem* **2015**, *8* (15), 2455.

(14) Nelson, A. M.; Long, T. E. *Polym. Int.* **2012**, *61* (10), 1485.

(15) Fu, K.-Y.; Cheng, Y.-H.; Chio, C.-P.; Liao, C.-M. *Environ. Sci. Pollut. Res.* **2016**, *23* (19), 19897.

(16) *Market Report Global Epoxy Resin Market*, 2nd ed.; Acmite Market Intelligence: Ratingen, Germany, 2014 .

(17) Auvergne, R.; Caillol, S.; David, G.; Boutevin, B.; Pascault, J. P. *Chem. Rev.* **2014**, *114* (2), 1082.

(18) Fache, M.; Darroman, E.; Besse, V.; Auvergne, R.; Caillol, S.; Boutevin, B. *Green Chem.* **2014**, *16*, 1987.

(19) Over, L. C.; Grau, E.; Grelier, S.; Meier, M. A. R.; Cramail, H. *Macromol. Chem. Phys.* **2017**, *218* (8), 1600411.

(20) Ferdosian, F.; Yuan, Z.; Anderson, M.; Xu, C. *Ind. Crops Prod.* **2016**, *91*, 295.

(21) van de Pas, D. J.; Torr, K. M. *Biomacromolecules* **2017**, *18*, 2640.

(22) Xin, J.; Li, M.; Li, R.; Wolcott, M. P.; Zhang, J. *ACS Sustainable Chem. Eng.* **2016**, *4* (5), 2754.

(23) Jung, J.; Park, C.; Lee, E. *J. Wood Chem. Technol.* **2017**, *37*, 433.

(24) Adler, E. *Wood Sci. Technol.* **1977**, *11*, 169.

(25) Yue, F.; Lu, F.; Ralph, S.; Ralph, J. *Biomacromolecules* **2016**, *17* (6), 1909.

(26) Crestini, C.; Melone, F.; Sette, M.; Saladino, R. *Biomacromolecules* **2011**, *12* (11), 3928.

(27) Crestini, C.; Lange, H.; Sette, M.; Argyropoulos, D. *Green Chem.* **2017**, *19*, 4104.

(28) Prat, D.; Wells, A.; Hayler, J.; Sneddon, H.; McElroy, C. R.; Abou-Shehada, S.; Dunn, P. J. *Green Chem.* **2015**, *17* (10), 4848.

(29) Jawerth, M.; Johansson, M.; Lundmark, S.; Gioia, C.; Lawoko, M. *ACS Sustainable Chem. Eng.* **2017**, *5*, 10918.

(30) Gierer, J.; Lindeberg, O. *Acta Chem. Scand.* **1979**, *33*, 580.

(31) Capanema, E.; Balakshin, M.; Katahira, R.; Chang, H.; Jameel, H. *J. Wood Chem. Technol.* **2015**, *35*, 17. Zhang, L.; Gellerstedt, G. *Magn. Reson. Chem.* **2007**, *45*, 37.

(32) Majtnerova, A.; Gellerstedt, G. *Nord. Pulp Pap. Res. J.* **2006**, *21* (1), 129.

(33) Gierer, J. *Wood Sci. Technol.* **1980**, *14* (4), 241.

(34) Salanti, A.; Zoia, L.; Orlandi, M. *Green Chem.* **2016**, *18* (14), 4063.

(35) Huang, L.-H.; Shih, Y.-C.; Wang, S. – H.; Kuo, P.-L.; Teng, H. *J. Mater. Chem. A* **2014**, *2*, 10492.

(36) Mc Aninch, I. M.; Palmese, G. R.; Lenhart, J. L.; La Scala, J. J. *Polym. Eng. Sci.* **2015**, *55* (12), 2761.

(37) Stutz, H.; Illers, K. – H.; Mertes, J. J. *J. Polym. Sci., Part B: Polym. Phys.* **1990**, *28* (9), 1483.

(38) Rietsch, F.; Daveloose, D.; Froelich, D. *Polymer* **1976**, *17* (10), 859.

(39) Lee, T. M.; Ma, C. C. M.; Hsu, C. W.; Wu, H. L. *Polymer* **2005**, *46*, 8286.

(40) Erman, B.; Mark, J. E. *Structures and properties of rubberlike networks*; Oxford University Press: Oxford, 1997.

(41) Maiorana, A.; Ren, L.; Lo Re, G.; Spinella, S.; Ryu, C. Y.; Dubois, P.; Gross, R. A. *Green Mater.* **2015**, *3* (3), 80.

DOI: 10.1021/jacs.7b13620
J. Am. Chem. Soc. 2018, 140, 4054–4061